LEVEL DENSITY PARAMETER OF NUCLEI AT FINITE TEMPERATURE [1]

C.Gregoire [2], T.T.S.Kuo, D.B.Stout

Physics Department, State University of New York at Stony Brook, Stony Brook,

NY 11794-3800, USA

November 12, 1989

ABSTRACT

The contribution of particle-particle (hole-hole) and of particle-hole ring diagrams to the nuclear level density parameter at finite temperature is calculated. We first derive the correlated grand potential with the above ring diagrams included to all orders by way of a finite temperature RPA equation. An expression for the correlated level density parameter is then obtained by differentiating the grand potential. Results obtained for the ^{40}Ca nucleus with realistic matrix elements derived from the Paris potential are presented. The contribution of the RPA correlations is found to be important, being significantly larger than typical Hartree-Fock results. The temperature dependence of the level density parameter derived in the present work is generally similar to that obtained in a schematic model. Comparison with available experimental data is discussed.

I.Introduction

Collective and pairing vibrations are known to be important for the ground state properties of nuclei [1]. The first are conveniently described by the particle-hole random phase approximation (RPA), the second being obtained by the particle-particle (hole-hole) RPA. Indeed, the amplitudes of these vibrations are provided together with their energies by solving the respective RPA equations using either empirical or realistic residual interactions. For a ^{40}Ca nucleus at zero temperature,

the correlation energies due to core polarizations are of the order of 10 MeV. The extension of RPA equations to finite temperature systems allows us to extract the grand potential and hence relevant thermodynamical observables. Since particles and holes overlap around the Fermi surface, one should expect a gradual disappearance of the correlation contribution from polarizations as temperature increases.

The level density around the Fermi surface is among the key quantities in the statistical model for the de-excitation of hot nuclei. It can be characterized by an effective level density parameter $a_{eff} = \frac{E(T)-E(0)}{T^2}$ where T is the temperature and E the total energy [2]. The empirical value for a_{eff} is about $\frac{A}{8}$ at low temperature, A being the mass number. On the other hand, recent experimental studies seem to indicate a transition of a_{eff} from $\frac{A}{8}$ to $\frac{A}{13}$ in the temperature range between 2 and 5 MeV [3]. In Hartree-Fock calculations, this level density parameter at finite temperature has been obtained from the grand potential after subtraction of the continuum [4]. As a matter of fact, solutions of the finite temperature Hartree-Fock problem for temperatures exceeding 8-10 MeV seems to have not been carried out. Below this temperature range, the semi-classical calculations of ref [5] show that the level density parameter does vary slightly with temperature from $\frac{A}{9}$ at T=1 MeV to $\frac{A}{11}$ at T=5 MeV. This tiny dependence is due to the enhanced diffusivity of the surface for increasing temperature.

The aim of this paper is to calculate the RPA contributions to the effective level density parameter with a realistic effective interaction. More specifically we want to study the correlation effect to the level density parameter a_{eff}, generated by the particle-particle (hole-hole) , to be denoted from now on as pphh, ring diagrams and the particle-hole (ph) ring diagrams. Previous calculations [6,7,8] have studied these diagrams either with schematic forces or in the framework of a schematic model. Their qualitative conclusion is that the ph RPA contribution to the level density is small. It vanishes for temperatures larger than 4 MeV. The pphh RPA contribution is much larger with a weaker temperature dependence. On the other hand, the contributions from 2p-1h and 1p-2h correlations have also been calculated in ref[9], and are found to be significant. A comparison between the result of ref[10] and the

schematic model results of ref[8] is hard to establish because the approximations and technical methods employed are too different. Nevertheless, as pointed out in ref [11,6,12], one should expect from collective and pairing vibrations an enhancement of the effective mass near the Fermi level. Since the level density parameter is proportional to the effective mass [13], an increase of the level density parameter above the Hartree-Fock value is expected at low temperature. At high temperature, the particles and the holes being less and less distinguishable the extra-contribution from the correlations should disappear. A precise microscopic calculation was highly desirable from a two-fold point of view. Firstly, new experimental data about hot nuclei properties become available with intermediate energy heavy ion facilities.. Secondly, the effective level density provides us with the heat capacity of nuclear systems. It is of prime importance in the collapse and the eventual bounce-off of stars since the removed thermal energy is no longer available as mechanical energy [14,15].

Our philosophy to perform these calculations is to make:

i) An exhaustive account of the contribution of bubble and ladder diagrams to the grand potential for hot nuclei, carried out in a Green's function framework. This allows us to sum up the ring diagrams for pp(hh) and ph excitations at finite temperature to all orders[16,17]. This procedure has already been applied to nuclear matter properties, and was found to be very powerful. [18]

ii) A realistic calculation of the residual interaction matrix elements. In the present work, we use Brueckner reaction matrix elements derived from the Paris nucleon-nucleon potential using harmonic oscillator basis wave functions. The model-space projection operator involved in the G-matrix calculation will be treated accurately. [19]

iii) A determination of the ring-diagram summation via the solution of the RPA equations. The grand potential is in turn deduced from the ring diagram expression. A differentiation with respect to the inverse temperature allows us to obtain the total energy at finite temperature and hence the level density parameter.

In the following we shall first describe, in Section II, the formalism involved in the summation of the finite temperature ring diagrams. Some details of the G-matrix

calculations of the residual interaction will also be given. The expressions for the effective level density parameter are derived. Section III presents our first results. As an illustration, we discuss the temperature dependence of the level density parameter for the ^{40}Ca nucleus up to 7 MeV.

II. Formalism.

In this section, we wish to describe our formalism for calculating the level density parameter with the correlation effect from the pphh and ph ring diagrams included to all orders. We start from the thermodynamic potential Ω. A first step is to calculate Ω with the inclusion of the above ring diagrams. A general and rather powerful framework for doing so has already been worked out by several authors [20,8,16,17], and we will follow it closely in the present work. In order to explain our calculation with adequate detail , especially to explain some subtle differences between the pphh and the ph ring- diagram contributions, we need to repeat first some of its essential steps, in particular with respect to the so-called eigenvalue (EV) method which we will employ in the present work in summing up the ring diagrams of Ω.

The thermodynamic potential Ω can be written as $\Omega = \Omega_0 + \Omega_{int}$ where Ω_0 is the unperturbed part of Ω corresponding to H_0, the non-interacting hamiltonian. We write the nuclear hamiltonian as $H=H_0+H_1=(T+u)+(V-u)$, where T and V denote respectively the kinetic energy and the two-body nucleon-nucleon (NN) interaction term and u is a chosen one-body potential such as that of a harmonic oscillator. Consider for the time being that V is a well behaved effective NN interaction. (As to be discussed later actual calculations will be carried out using a G-matrix interaction.) It is well known that the interacting thermodynamic potential Ω_{int} can be expressed as a linked diagram expansion in terms of H_1. We would like to sum up certain classes of ring diagrams of Ω_{int}, and this can in fact be performed rather conveniently as described in the following.

II.A. pphh ring diagrams

Here we consider specifically the all-order sum of the pphh ring diagrams as illustrated in Fig. 1. This sum is denoted as Ω_{int}^{pp} and can be written as [16,17]

$$\Omega_{int}^{pp} = \frac{1}{\beta} \sum_{\nu} e^{i\omega_{\nu}o^{+}} \text{tr}\{FV - \frac{1}{2}(FV)^{2} + \frac{1}{3}(FV)^{3} - ...\} \tag{1}$$

where F is the pair propagator

$$F_{ij}(i\omega_{\nu}) = \begin{cases} -\frac{\bar{f}_i\bar{f}_j - f_i f_j}{i\omega_{\nu} - (\bar{\epsilon}_i + \bar{\epsilon}_j)}, & \bar{\epsilon}_i + \bar{\epsilon}_j \neq 0 \\ \beta f_i f_j \delta_{\nu 0}, & \bar{\epsilon}_i + \bar{\epsilon}_j = 0. \end{cases} \tag{2}$$

Here f_k is the Fermi-Dirac distribution function and $\bar{f}_k = 1 - f_k$. As usual we define $\bar{\epsilon}_k \equiv \epsilon_k - \mu$, where ϵ_k is the single-particle energy and μ the chemical potential. The Matsubara frequency is $\omega_{\nu} = 2\nu\pi/\beta$ with $\nu = 0, \pm 1, \pm 2, ...$ and $\beta = 1/k_B T$ with k_B the Boltzmann constant and T the temperature. In Eq. 1, V stands for the antisymmetrized matrix element of the interaction, $V_{ijkl} = -V_{jikl}$, and the pp(or hh) labels are to be summed over $i > j$ and $k > l$.

The counting factors 1, 1/2, 1/3 and so forth in Eq. 1 play an important role here and they are determined from the symmetry properties of the ring diagrams. For example the third order term has a well-known factor 1/3! originated from the linked diagram expansion of the thermodynamic potential. Using Hugenholtz antisymmetrized vertices, there are two topologically equivalent third order pphh ring diagrams. Hence 2 times 1/3! gives 1/3. By virtue of these counting factors, the series involved in Eq.1 is a logarithmic series. To facilitate its calculation let us rewrite it as

$$\Omega_{int}^{pp} = -\frac{1}{\beta} \sum_{\nu} e^{i\omega_{\nu}o^{+}} \ln\{\det[G^{pp}(i\omega_{\nu})F(i\omega_{\nu})^{-1}]\} \tag{3}$$

where G^{pp} is the finite-temperature Green's function

$$G^{pp}(i\omega_{\nu}) = F(i\omega_{\nu}) - F(i\omega_{\nu})VG^{pp}(i\omega_{\nu}). \tag{4}$$

We now introduce a RPA-type equation

$$\sum_{k>l}\{(\bar{\epsilon}_i + \bar{\epsilon}_j)\delta_{ij,kl} + Q(ij)V_{ijkl}\} < kl|\chi_n > = \Delta_n < ij|\chi_n > \tag{5}$$

where $Q(ij)$ stands for $(\bar{f}_i \bar{f}_j - f_i f_j)$. The $\tilde{\chi}$ vectors are defined by the biorthonormal relations $< \tilde{\chi}_m | \chi_n > = \delta_{mn}$. In fact $< \tilde{\chi}_m | ij > = \pm < \chi_m | ij > / Q(ij)$ with the normalization $\sum_{i<j} | < ij | \chi_n > |^2 / Q(ij) = \pm 1$, where the upper (lower) sign refers to states dominated by particle-particle (hole-hole) components. Let us consider the case with $\bar{\varepsilon}_i + \bar{\varepsilon}_j \neq 0$ and $\Delta_n \neq 0$. [1] The Lehmann representation of G^{pp} is then

$$G^{pp}_{ijkl}(i\omega_\nu) = \sum_{n(\Delta_n \neq 0)} < ij | \chi_n > < \tilde{\chi}_n | kl > \frac{f_k f_l - \bar{f}_k \bar{f}_l}{i\omega_\nu - \Delta_n} \tag{6}$$

where χ_n and Δ_n are given by Eq. 5

From Eqs.2 and 6 we have

$$[G^{pp}(i\omega_\nu)F(i\omega_\nu)^{-1}]_{ijkl} = \sum_{n=1}^{N} W_{ij}(n)Z_{kl}(n) \tag{7}$$

with

$$W_{ij}(n) \equiv \frac{< ij | \chi_n >}{i\omega_\nu - \Delta_n}, \quad Z_{kl}(n) \equiv < \tilde{\chi}_n | kl > (i\omega_\nu - \bar{\varepsilon}_{kl}). \tag{8}$$

For brevity we shall from now on use the abbreviated notation $\bar{\varepsilon}_{kl}$ for $\bar{\varepsilon}_k + \bar{\varepsilon}_l$. Note that the total number of ij states $(i > j)$ is also N and similarly for kl. Hence the above can be written in matrix form and we obtain

$$\det[G^{pp}F^{-1}] = \frac{\prod_{i>j}(i\omega_\nu - \bar{\varepsilon}_{ij})}{\prod_n(i\omega_\nu - \Delta_n)} \det \begin{pmatrix} 1 & 0 & \dots & 0 \\ 0 & 1 & \dots & 0 \\ \vdots & \vdots & \ddots & \vdots \\ 0 & 0 & \dots & 1 \end{pmatrix} \tag{9}$$

where we have made use of the relation $< \tilde{\chi}_m | \chi_n > = \delta_{mn}$. Substituting the above into Eq. 3 and noting the identities

$$\ln \frac{i\omega_\nu - a}{i\omega_\nu - b} = \frac{1}{2} \int_{-1}^{1} \frac{(b-a)d\xi}{i\omega_\nu - \frac{1}{2}[(b+a) - \xi(b-a)]} \tag{10}$$

---

[1]The calculations considered here are for finite nuclei and we employ a discrete single particle spectrum. Thus the situation where $\bar{\varepsilon}_i + \bar{\varepsilon}_j$ and Δ_n are precisely zero does not occur in actual calculations.

and

$$\frac{1}{\beta} \sum_{\nu} e^{i\omega_\nu 0^+} \frac{1}{i\omega_\nu - x} = \frac{-1}{e^{\beta x} - 1},$$ (11)

we obtain the compact and rather useful result

$$\Omega_{int}^{pp} = \frac{1}{\beta} \ln \frac{\Pi_n (1 - e^{-\beta \Delta_n})}{\Pi_{i>j}(1 - e^{-\beta \varepsilon_{ij}})}.$$ (12)

In deriving the above, we have also used the relation $\int [a + be^{mx}]^{-1} dx = [mx - \ln(a + be^{mx})]/am$. The above expression , which is rigorous, has been referred to as the EV method [17] for calculating Ω_{int}^{pp}. It has a rather transparent physical meaning; it is the difference between the grand potential obtained with RPA bosons and that obtained by treating unperturbed fermion pairs as bosons. This clearly gives the effect of the ring diagram correlation.

It is well known that the level density parameter is related to the thermal excitation energy $E^* = E(T) - E(0)$ where $E(T)$ and $E(0)$ are respectively the nuclear internal energies at temperatures T and 0.[8] The internal energy can be obtained from the thermodynamic potential, namely $E(T) = \frac{\partial}{\partial \beta}(\beta \Omega)$. To separate out the correlation effect, we write the internal energy as

$$E(T) = E_{HF}(T) + E_{cpp}(T) + E_{cph}(T)$$ (13)

where the subscripts refer, respectively, to Hartree-Fock, correlation from the pphh ring diagrams and correlation from the ph ring diagrams. The ph ring diagrams will be treated in the next section. The first-order pphh ring diagram, i.e. diagram (a) of Fig.1, is intended to be contained in $E_{HF}(T)$. Hence it has to be removed from the pphh ring-diagram sum of Eq. 12. This gives

$$E_{cpp}(T) = \frac{\partial}{\partial \beta}[\ln \frac{\Pi_n (1 - e^{-\beta \Delta_n})}{\Pi_{i>j}(1 - e^{-\beta \varepsilon_{ij}})} - \beta \sum_{i>j} f_i f_j V_{ijij}]$$ (14)

which leads to

$$E_{cpp}(T) = \sum_n B(\beta, \Delta_n)\Delta_n - \sum_{i>j} B(\beta, \varepsilon_{ij}) \varepsilon_{ij} \cdot \sum_{i>j} f_i f_j [1 - \beta(\varepsilon_i \bar{f}_i + \varepsilon_j \bar{f}_j)] V_{ijij}$$ (15)

where the B's are the Bose-Einstein distribution functions

$$B(\beta,\omega) = \frac{1}{e^{\beta\omega} - 1}. \tag{16}$$

The appearance of the B functions in Eq. 15 gives it a clear physical meaning; its first term is just the thermal average energy of the RPA bosons while the second term that of the noninteracting fermion pairs treated as bosons.

It must be pointed out that we have made an approximation in deriving Eq.15 from Eq.14. The approximation is that we have set $\partial\Delta_n/\partial\beta=0$ and $\partial\epsilon_i/\partial\beta=0$. These derivatives can be calculated numerically. They are, however, found to be generally small and thus we have chosen to neglect in Eq.15 the terms involving these derivatives. We are doing finite nuclei calculations and employ a discrete single particle spectrum. Futhermore we consider primarily temperatures which are low compared with major shell separations. Under these circumstances these derivatives are in fact expected to be small as we have numerically found.

In the limit of zero temperature Eq.15 becomes

$$E_{cpp}(0) = - \sum_{\Delta_n<0} \Delta_n + \sum_{i<j,\epsilon_{ij}<0} \epsilon_{ij} - \sum_{i<j<k_F} V_{ijij} \tag{17}$$

which is a familiar expression. With the above results, we can now calculate the level density parameter $a(T)$. We write it as

$$a(T) = \frac{E^-(T)}{T^2} = a_{HF}(T) + a_{cpp}(T) + a_{cph}(T). \tag{18}$$

The correlation contribution from the pphh ring diagrams is then given in terms of Eqs.15 and 17 as

$$a_{cpp}(T) = \frac{E_{cpp}(T) - E_{cpp}(0)}{T^2}. \tag{19}$$

II.B. ph ring diagrams

We now proceed to calculate the third term of Eq.18, the contribution from the ph ring diagrams. Let us consider the series of the ph ring diagrams shown in Fig.2 and denote its all order sum as S_{ph}. This series may be written as

$$S_{ph} = -\frac{1}{2\beta} \sum_{\nu} e^{i\omega_{\nu}o^{+}} \text{tr}\{\bar{F}\bar{V} + \frac{1}{2}(\bar{F}\bar{V})^2 + \frac{1}{3}(\bar{F}\bar{V})^3 + \ldots\} \tag{20}$$

where $\bar{F}$ is the particle-hole propagator

$$\bar{F}_{ij}(i\omega_{\nu}) = \begin{cases} -\frac{\bar{f}_i f_j - f_i \bar{f}_j}{i\omega_{\nu} - (\bar{\epsilon}_i - \bar{\epsilon}_j)}, & \bar{\epsilon}_i - \bar{\epsilon}_j \neq 0 \\ \beta f_i \bar{f}_j \delta_{\nu 0}, & \bar{\epsilon}_i - \bar{\epsilon}_j = 0. \end{cases} \tag{21}$$

The structure of Eq.20 is nearly identical to that of Eq.1; the essential difference is the overall factor of 2 in front of the summation. This comes from the counting of the topologically equivalent ph ring diagrams. [1] The all order sum of the ph ring diagrams can be carried out in a way very similar to our treatment of the pphh ring diagrams. Let us define the ph finite temperature Green function and the corresponding RPA equation as:

$$G^{ph}(i\omega_{\nu}) = \bar{F}(i\omega_{\nu}) + \bar{F}(i\omega_{\nu})\bar{V}G^{ph}(i\omega_{\nu}), \tag{22}$$

and

$$\sum_{kl}\{(\bar{\epsilon}_i - \bar{\epsilon}_j)\delta_{ij,kl} + (-\bar{f}_i f_j + f_i \bar{f}_j)\bar{V}_{ijkl}\} < kl|\chi_n > = \Gamma_n < ij|\chi_n > . \tag{23}$$

Here $\bar{V}$ is the particle-hole matrix element, namely $\bar{V}_{ijkl} = V_{ilkj}$. Using the above and the procedures of the previous section we obtain

$$S_{ph} = \frac{1}{2\beta} \ln \frac{\prod_n (1 - e^{-\beta\Gamma_n})}{\prod_{ij}(1 - e^{-\beta(\bar{\epsilon}_i - \bar{\epsilon}_j)})}. \tag{24}$$

It may be pointed out that S_{ph} is not yet the appropriate quantity for evaluating $a_{cph}(T)$ of Eq.18. There is some overcounting in the sum S_{ph} which needs to be removed. In the linked diagram expansion of Ω_{int} there is only one first order diagram

---

[1]Consider for example the third order ph ring diagram. It can be enumerated that there are altogether 64 topologically equivalent such ring diagrams. We use antisymmetrized vertices and thus there is a factor $(1/4)^3$ from the three interaction operators in the second quantized representation. Finally there is a factor 1/3! form the linked diagram expansion of the thermodynamic potential. Hence the net counting factor is 1/6 for the third order ph ring diagram as appeared in Eq.20.

which has already been taken care of by diagram (a) of Fig.1 as a pphh ring diagram. The second order diagram (2) of Fig.2 is identical to diagram (b) of Fig.1 which has already been included in Ω_{int}^{pp}. Thus we should explicitly remove diagrams (1) and (2) from S_{ph}. These two diagrams can be evaluated using standard methods. The resulting thermodynamic potential from the ph ring diagrams is then

$$\Omega_{int}^{ph} = S_{ph}' - D_1 - D_2 \qquad (25)$$

with

$$D_1 = -\frac{1}{2}\sum_{ij} f_i \bar{f}_j \bar{V}_{ijij}, \qquad (26)$$

and

$$D_2 = \begin{cases} -\frac{1}{2}\sum_{ijkl} \bar{V}_{ijkl}\bar{V}_{klij} f_i \bar{f}_j \frac{[-f_k f_l + f_k f_l]}{\bar{\epsilon}_{ij} - \bar{\epsilon}_{kl}} & \bar{\epsilon}_{ij} \neq \bar{\epsilon}_{kl} \\ -\frac{\beta}{4}\sum_{ijkl} \bar{V}_{ijkl}\bar{V}_{klij} \bar{f}_i f_j f_k \bar{f}_l & \bar{\epsilon}_{ij} = \bar{\epsilon}_{kl}. \end{cases} \qquad (27)$$

In the above $\bar{\epsilon}_{ij}$ stands for $\bar{\epsilon}_i - \bar{\epsilon}_j$. The internal energy $E_{cph}(T)$ can be obtained from Ω_{int}^{ph}. Then the corresponding contribution to the level density parameter is given by

$$a_{cph}(T) = \frac{E_{cph}(T) - E_{cph}(0)}{T^2} . \qquad (28)$$

II.C. G — matrices and angular momentum coupling

To carry out the aforementioned ring-diagram summations involves first overcoming several technical obstacles. First of all, there is the familiar problem that the repulsive core of the nucleon-nucleon interaction is unsuitable for conventional Hartree-Fock and diagrammatic calculations. We proceed by replacing the nucleon-nucleon interaction V in the above formuli by a model-space Brueckner G-matrix. This has a two-fold advantage in that it a) takes into account the summation over high energy states and thereby allows us to carry out the calculations in a finite dimensional model space, and b) its matrix elements are well-behaved. We note that

it is important to treat the projection operator in the G matrix accurately so that there will be no overcounting between the correlations included in the G matrix and those included in the pphh ring diagrams.

The model-space G-matrix is defined as

$$G(\omega) = V + V\frac{Q_{2p}}{\omega - H_0(2p)}G(\omega) \tag{29}$$

where Q_{2p} is the two-particle (2p) projection operator for all such states outside the the model space. Its complement projection operator is P_{2p}, satisfying

$$P_{2p} + Q_{2p} = I_{2p} = \sum_{\text{all}} |ij\rangle\langle ij| . \tag{30}$$

The model-space used in the present work is specified in fig.3, with (n_1, n_2, n_3) given by (6,15,28).[19] Note that the single-particle Hamiltonian is contained in the definition of the G-matrix Eq.29. As the intermediate states involved in the G-matrix are predominantly of high excitation energies, we make the reasonable physical choice that the single-particle spectrum H_0 for the Q-space may be replaced by the free kinetic spectrum T. Thus, the G-matrix equation becomes

$$G_T(\omega) = V + VQ_{2p}\frac{1}{Q_{2p}(\omega - T)Q_{2p}}Q_{2p}G_T(\omega). \tag{31}$$

In practice, the solution of the G-matrix Eq.31 remains rather difficult, and there are a host of approximations (e.g. angle average) designed to simplify its solution. The basic difficulty resides in the fact that the nucleon-nucleon interaction V is diagonal in the center of mass frame, while the lab frame Q-space projection operator is not, thus hampering the solution of Eq.31. Rather than employ one of the standard approximations, we numerically solved the equation according to the formally exact technique of Tsai and Kuo [21].

We sketch their derivation of the formula we used as follows. First one notes that Eq.31 may be rewritten as

$$G_T(\omega) = V + VQ_{2p}\frac{1}{Q_{2p}(\omega - T(2p) - V)Q_{2p}}Q_{2p}V . \tag{32}$$

Next they proved the simple matrix identity [21]

$$Q\frac{1}{QAQ}Q = \frac{1}{A} - \frac{1}{A}P\frac{1}{P(1/A)P}P\frac{1}{A} \ .$$ (33)

Applying this identity to Eq.32, we obtain

$$G_T(\omega) = G_{TF}(\omega) + \Delta G(\omega)$$ (34)

where G_{TF} is the free G-matrix defined with respect to the kinetic energy single-particle Hamiltonian

$$G_{TF} = V + V\frac{1}{\omega - T(2p)}G_{TF}(\omega) \ .$$ (35)

$\Delta G(\omega)$ is a correction term defined entirely within the P-space, given as

$$\Delta G(\omega) = -V\frac{1}{A}P_{2p}\frac{1}{P_{2p}(1/A)P_{2p}}P_{2p}\frac{1}{A}V$$

$$A \equiv \omega - T(2p) - V \ .$$ (36)

Using the definition for G_{TF} one readily obtains an expression more convenient for calculation, namely

$$\Delta G(\omega) = -G_{TF}(\omega)\frac{1}{e}P_{2p}\frac{1}{P_{2p}[(\frac{1}{e}) + (\frac{1}{e})G_{TF}(\frac{1}{e})]P_{2p}}P_{2p}\frac{1}{e}G_{TF}(\omega)$$

$$e \equiv \omega - T(2p) \ .$$ (37)

Thus we see that the G-matrix is now expressed as the sum of two terms; the first term is the free G-matrix while the second is calculated using only some simple model-space matrix operations involving the free G-matrix. The free G-matrix no longer contains the troublesome Q-space projection operator and may be calculated via momentum-space matrix-inversion methods [22]. Indeed the above formalism provides a convenient and essentially exact method for calculating the model-space G-matrix. Of course, one might question the validity of using the zero temperature G-matrix in a finite temperature calculation. However, it should be clear that if the n_2 cutoff is defined at an energy which is large compared to the temperature under consideration, then the zero-temperature G-matrix should remain applicable in the

finite temperature case as well. A more careful analysis [16] upholds this intuitive assessment.

Accurate G-matrix calculations of the above type have been carried out in the past only for light nuclei. For example, the calculation performed by Krenciglowa et al. [19] was for the s-d shell nuclei and employed a model space of $(n_1, n_2, n_3) =$ (3,10,21). The model space of (6,15,28) used in the present work is much larger and consequently the calculation involved is considerably more extensive. A number of improvements have been implemented in our earlier G-matrix programs[19] in order to carry out the present calculation.

Another point of technical interest is the calculation of the ph matrix elements. Our G-matrix elements are calculated in the form of particle-particle matrix elements. To determine the ph-matrix elements we use the familiar relation [23]

$$\langle ad^{-1}JM|G|cb^{-1}JM\rangle = -\sum_{J'}(2J'+1) \times \left\{ \begin{array}{ccc} a & d & J \\ c & b & J' \end{array} \right\} \langle abJ'M'|G|cdJ'M'\rangle \quad (38)$$

where { } is the six-j symbol. The matrix element on the left-hand side denotes the ph matrix element while that on the right-hand side the particle- particle matrix element.

III.Results and discussion

As a first application of the previous formalism, we consider a rather light nucleus, ^{40}Ca, for which computations can be performed relatively easily. Its single particle spectrum at zero temperature can be deduced from the spectra of mass 39 and mass 41 nuclei. The 2s1d shell and the 2p1f shell which are located just below and above the Fermi level define our model space where particle-particle, hole-hole and particle-hole configurations are built. As a matter of fact, the single particle energy spectrum employed here is identical to the one given in figure 1 of ref[7]. Taking advantage of the very weak temperature dependence of the single particle levels which can be inferred from hot Hartree-Fock calculations [4], we have assumed that

the spectrum at zero temperature is unchanged up to 6 MeV. On the other hand, the chemical potential has been calculated for each temperature value in order to conserve the particle number in the Hartree-Fock approximation. One should notice that a correction should be applied when RPA correlations are included. Nevertheless, we assume that the effective level density parameter should not be so sensitive to such a correction. For the ^{40}Ca calculation reported here, we have checked numerically that small adjustments of the finite temperature chemical potential do not significantly modify our results. Our calculations have been performed by including all the states with positive and negative parities for J ranging from 0 to 5. In the particle-hole case the 1^- state with T=0 which corresponds to a spurious excitation was excluded from our calculation.

The effective level density parameter calculated in the present work is displayed in figure 4. Curve C shows the temperature dependence of the ph contribution calculated according to Eqs.25 to 28. Curve B gives the pp(hh) contribution. And finally, Curve A represents the total contribution of the RPA correlations to the level density. One can observe a rather smooth temperature decrease of the ph contribution, whereas the pp(hh) one is more pronounced. The absolute value of the ph contribution is more than 3 times smaller than the pairing vibration one. This later one is very large in magnitude. Below 3 MeV, its absolute value is of the same order of magnitude as the Hartree-Fock one, which was estimated in a semi-classical approximation to be equal to 4.5 MeV^{-1} at temperature 2 MeV [24]. In fact, the experimental level density parameter is equal to 6-7 MeV^{-1} in the ^{40}Ca region[25]. In other words the sum of the Hartree-Fock plus correlations seems to overpredict the absolute value of the level density parameter. Nevertheless the calculated values have the same general temperature dependence as the experimental results of ref[3]. Since the experiments reported in this reference were performed for much heavier nuclei with a mass equal to around 160, a direct comparison is not very meaningful. For the particle-hole contribution, our calculation exhibits temperature dependence similar to that given by the semi-classical estimate [9]. On the other hand, the schematic model estimates exhibit a much sharper[26] temperature dependence. For

the particle-particle (hole-hole) contribution, our results confirm those obtained for the ^{208}Pb nucleus in ref[8] as far as the temperature dependence is concerned. Our comparatively larger results (after scaling by the nucleus mass number) have probably their origin in the residual interaction. A detailed analysis would require a systematic study along the nuclei chart which is out of the scope of this first calculation.

IV.Conclusion

We have addressed the question of the temperature dependence of the level density parameter for nuclei. The summation of ring diagrams allows us to calculate the grand potential and related thermodynamical quantities. In particular, correlation energies at finite temperature are deduced. The procedure for performing these calculations is as follows: i) the single- particle spectrum is determined for each nucleus from experimental observations of levels for neighbouring nuclei. ii) matrix elements of the residual interaction are determined from a realistic nucleon-nucleon potential for every pp, hh or ph configuration. iii) the finite temperature RPA equations for ph and pphh states with given quantum numbers are solved. The involved configurations are those with a given angular momentum J and parity π. iv) The correlation energies are calculated from expressions obtained by way of the grand potential. It was shown that these can be expressed as functions of the RPA eigenvalues, the single particle energies and the temperature. For the first time, we have applied the previous procedure using the realistic nucleon-nucleon Paris potential. The matrix elements have been obtained in the relevant model space for a ^{40} Ca nucleus. It is found that the pphh contribution is more than three times larger than the ph one. At variance to the results of the schematic model [8], the temperature dependence of the pphh contribution is rather violent between 3 and 5 MeV. The level density parameter drops down in this domain. These findings, which should be firmly sustained by systematic calculations, could have drastic consequences, as far as nuclear models are concerned. Two examples can be given. The first one deals with collapse calculations

in stars. The thermal pressure governs to a large extent the collapse process [14]. The propagation of the shock wave should be much affected by a strong temperature dependence of the effective mass, i.e. of the effective level density parameter. The second example is given by the studies of the multifragmentation decay of highly excited nuclei [2]. Among the key ingredients of the statistical approaches is obviously the amount of thermal excitation energy stored inside the fragments. Results obtained by various groups differ in a large extent because of different prescriptions for the temperature dependence of the level density parameters. We hope that our results will help to clarify the situation.

References

[1] A.Bouyssy and N.Vinh-Mau, Nucl. Phys. A229, 1 (1974).

[2] E.Suraud, C.Gregoire, and B.Tamain [Ganil P89-04, to appear in Progress in Nuclear and Particle Science].

[3] R.Wada et al., Nucl. Phys. A471, 351c (1987).

[4] P.Bonche, S.Levit, and D.Vautherin, Nucl. Phys. A427, 278 (1984).

[5] E.Suraud, P.Schuck, and R.W.Hasse, Phys. Lett. 164B, 212 (1985).

[6] P.F.Bortignon and C.H.Dasso, Phys. Lett. B179, 313 (1986).

[7] D.Vautherin and N.Vinh-Mau, Nucl. Phys. A422, 140 (1984).

[8] N.Vinh-Mau, Nucl. Phys. A491, 246 (1989).

[9] R.W.Hasse and P.Schuck, Phys. Lett. B179, 313 (1986).

[10] N.Vinh-Mau and D.Vautherin, Nucl. Phys. A445, 245 (1985).

[11] P.Grange, J.Cugnon, and A.Lejeune, Nucl. Phys. A473, 365 (1987).

[12] M.Prakash, J.Wambach, and Z.Y.Ma, Phys. Lett. B128, 141 (1983).

[13] M.Barranco and J.Treiner, Nucl. Phys. A351, 261 (1981).

[14] E.Baron, Phys. Rep. 163, 37 (1988).

[15] J.Lattimer [private communication].

[16] S.D.Yang and T.T.S.Kuo, Nucl. Phys A467, 461 (1987).

[17] S.D.Yang, M.F.Jiang, T.T.S.Kuo, and P.J.Ellis, Phys. Rev. C. 40C, 1085 (1989).

[18] M.F.Jiang, T.T.S.Kuo, and H.Muther. Phys. Rev. C38, 2408 (1988).

[19] E.M.Krenciglowa, C.L.Kung, T.T.S.Kuo, and E.Osnes, Ann. Phys. **101**, 154 (1976).

[20] D.Vautherin and N.Vinh-Mau, Phys. Lett. **120B**, 261 (1983).

[21] S.F.Tsai and T.T.S.Kuo, Phys. Lett. **38B**, 427 (1972).

[22] G.E.Brown, A.D.Jackson, and T.T.S.Kuo, Nucl. Phys. **A133**, 481 (1969).

[23] T.T.S.Kuo, J.Shurpin, K.C.Tam, E.Osnes, and P. Ellis, Ann. Phys. **132**, 237 (1981).

[24] E.Suraud, Nucl. Phys. **A462**, 109 (1987).

[25] A.Gilbert and A.G.W.Cameron, Can.J.Phys. **43**, 1446 (1965).

[26] D.Vautherin and N.Vinh-Mau, in *Windsurfing the Fermi Sea, Vol II.*, edited by T.T.S.Kuo and J.Speth, p. 213 (Elsevier Science, 1987).

FIGURE CAPTIONS

Fig.1 Some low-order pphh ring diagrams of Ω_{int}. Each dashed line represents a G-matrix vertex.

Fig.2 Some low order ph ring diagrams of S_{ph}.

Fig.3 G-matrix model-space used in the present work.

Fig.4 . Temperature dependence of the level density parameter for ^{40}Ca, calculated from the Paris potential. Line C: ph contribution (see text). Line B: pphh contribution. Line A: sum of ph and pphh contributions.
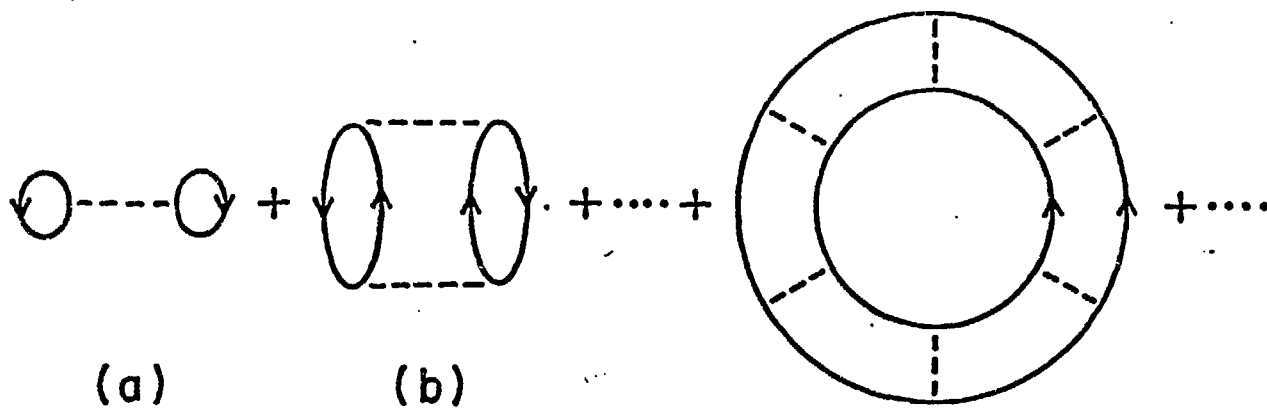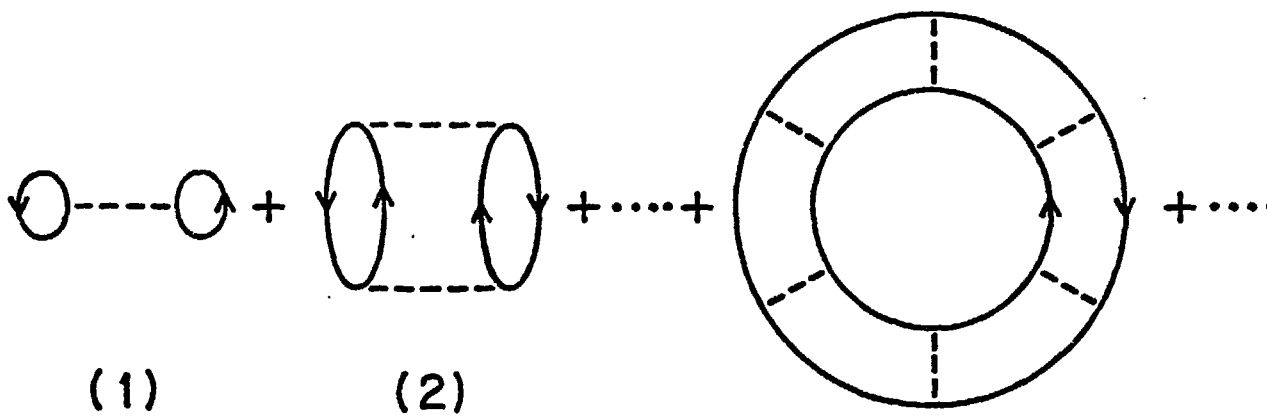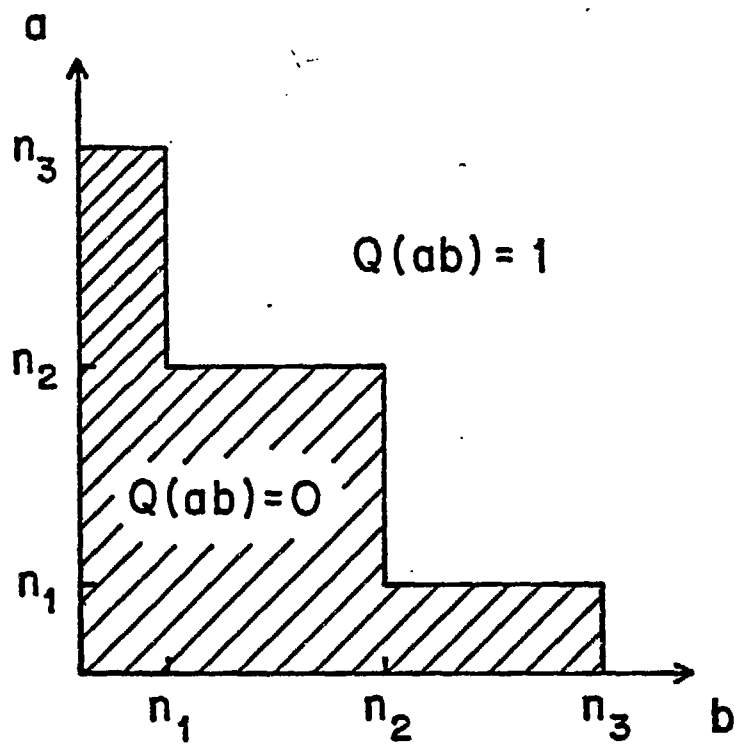
(a)   (b)

Fig. 1

(1)   (2)

Fig. 2

Fig. 3

Fig. 4